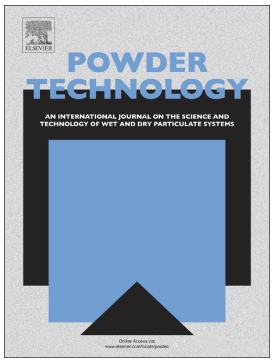

Comparison of granules obtained with two twin-screw granulators of different diameter working at the same shear rate

Nazareth E. Ceschan, María C. Balbi, Pablo Ravazzoli, German Drazer, Fernando Muzzio, Gerardo Callegari

PII: S0032-5910(25)00487-5

DOI: https://doi.org/10.1016/j.powtec.2025.121092

Reference: PTEC 121092

To appear in: *Powder Technology*

Received date: 15 February 2025

Revised date: 12 April 2025

Accepted date: 30 April 2025

Please cite this article as: N.E. Ceschan, M.C. Balbi, P. Ravazzoli, et al., Comparison of granules obtained with two twin-screw granulators of different diameter working at the same shear rate, *Powder Technology* (2024), https://doi.org/10.1016/j.powtec.2025.121092

Comparison of granules obtained with two twin-screw granulators of different diameter working at the same shear rate

Nazareth E. Ceschan[(1,2,)], María C. Balbi[(3)], Pablo Ravazzoli[(4)], German Drazer[(5,6)], Fernando Muzzio[(6,7)] and Gerardo Callegari[(6,7,*)]

[(1)]Departamento de Biología, Bioquímica y Farmacia, Universidad Nacional del Sur, Bahía Blanca, Buenos Aires, Argentina

[(2)]Planta Piloto de Ingeniería Química (UNS-CONICET), Bahía Blanca, Buenos Aires, Argentina

[(3)]Laboratorio de Caracterización de Partículas, Facultad de Ingeniería Química, Universidad Nacional del Litoral (UNL), Santa Fe, Santa Fe, Argentina

[(4)]Instituto de Física Arroyo Seco, Universidad Nacional del Centro de la Provincia de Buenos Aires; CIFICEN-CONICET-CICPBA, Tandil, Buenos Aires, Argentina,

[(5)]Mechanical and Aerospace Engineering, Rutgers University, Piscataway, NJ

[(6)]C-SOPS, Center for Structured Organic Particulate Systems. Piscataway, NJ.

[(7)]Department of Chemical and Biochemical Engineering, Rutgers, The State University of New Jersey, Piscataway, NJ.

* Corresponding author: Gerardo Callegari (g.callegari@rutgers.edu)

Abstract

We study the response of two twin-screw granulators of different barrel diameter to the variation of three process parameters (liquid-to-solid ratio, screw speed and throughput), while maintaining the same shear rate field along the screws. Various responses, including size distribution, porosity and content uniformity, were measured to determine granule characteristics. The set of experiments was based on a central composite design face-centered. Granules in both systems showed drug content consistent with expected values across varying process parameters. Relative granules size, normalized with the granulator gap, was larger for the equipment with the smaller gap. The liquid-to-solid ratio (LSR) was the most influential parameter affecting the granule size. Specifically, dimensional granule size increased with LSR values in both systems, consistent with previous studies. Elevated LSR values resulted in greater amounts of over-granulated material, whereas lower values produced exceedingly small (fines) or under-granulated material. The minimum amounts of both over- and under-granulated material were found at intermediate LSR values. Porosity varied differently between the systems, with a consistent reduction observed as LSR decreased from 0.3 to 0.4. Optimization studies revealed that central values of LSR and screw speed minimized fines and bigger granules while maximizing porosity, critical attributes for downstream processing. Granule size and porosity exhibited no significant correlation with tablet tensile strength across both systems. These findings offer valuable insights for optimizing pharmaceutical manufacturing processes to enhance product quality.

Keywords: twin screw granulator; granule properties; optimization; tabletability

1. Introduction

For over 50 years solid dosage forms, the most popular administration method, have been manufactured using a methodology known as batch production, an extensive process involving multiple discrete steps and the use of large-scale systems. After each step, production is typically halted for quality testing and the waiting times between production steps can significantly affect the production timeline. Alternatively, pharmaceutical products could be obtained through continuous manufacturing, an uninterrupted process in which raw materials are fed through a fully integrated assembly line, eliminating waiting times between steps. This method saves time, reduces human errors and drug shortages and can operate for longer periods to meet higher demand [1][2][3].

An important unit operation in the manufacturing of oral solid dosage forms is wet granulation (WG), typically used to improve critical material and product properties including flow, content uniformity, disintegration, dissolution and compressibility [4]. WG uses liquid as a binder to agglomerate fine particles into larger granules and both batch and continuous processes are available for wet granulation [4].

Twin screw granulators are especially well-suited for continuous pharmaceutical processes. Compared to other granulation technologies, twin screw granulation (TSG) allows for high drug loading and can process heat-sensitive materials with moderate energy requirements [4]. Screw elements (such as type, pitch and arrangement) and process parameters (e.g., screw speed, throughput, liquid-to-solid ratio and barrel temperature) can be selected depending on the application. These process parameters directly affect system parameters (working conditions) that in general cannot be controlled directly (such as power consumption, shear rate, powder feed number, specific mechanical energy, residence time distribution, fill level) [5][9][11][12]. Both, process and system parameters, impact the performance of the WG process and the final properties of the granules. The powder formulation also affects the granulation process and the selection of working parameters, such as the liquid-to-solid ratio (LSR). For example, hydrophobic drugs often require relatively high LSR values, in some cases up to 50% [6][5][7].

After wet granulation, a drying step is required. Traditionally, this step is conducted as a batch process and interrupts the continuous character of the granulation workflow. In contrast, integrating the drying process directly into the granulation workflow makes WG a truly continuous technique. While recent advancements have led to the development of systems incorporating in-barrel drying, it is important to note that these systems often necessitate high temperatures, limiting their applicability to thermally stable materials [8]. Some continuous drying system coupled to granulators are currently available. Therefore, the ability to transfer a process from widely used twin screw granulators to different ones that provide in-line drying systems is important to achieve continuous WG processes.

The use of different granulators can lead to variations in granule characteristics, even when maintaining constant formulation, screw design and process parameters [10] while transfer of system parameters often proves to be challenging. Previous research on TSG has studied different system parameters as responses, as reviewed by Lute et al. [9]. However, it is still a significant challenge to ensure consistent granule properties across different granulators or scales for WG methods. Among system parameters, powder feed number (PFN) and shear rate have been proposed as important parameters in TSG scale-up. PFN represents the rate at which powder is fed into the barrel of the processing system relative to the screw turnover volume [13], and is related to the fill level [9][11]. Osorio et al. found that PFN is more useful as

a scaling-out parameter (to increase the production rate) than to scale-up a process to a granulator of different dimensions. Shear stress depends on both the screw speed as well the rheological behavior of the granulated material. The shear stress exerted by the screw elements causes the wet mass to spread and create new interfaces, which aids in mixing and the shear rate measures the magnitude of this spreading process [5].

The aim of this study is to transfer the process between granulators of different scales without a specific focus on scaling up the process. For that, we compare the critical properties of ibuprofen granules produced by two different granulators designed for pharmaceutical applications. Ibuprofen, a hydrophobic model API extensively studied in WG processes [14], was granulated with a formulation that also includes lactose, microcrystalline cellulose and polyvinylpyrrolidone as excipients. Similar configurations were sought for both granulators. Screw speed, N, was adjusted to achieve comparable shear rates for both systems. Finally, liquid-to-solid ratio (LSR) and throughput (TP) were set to ensure an overlap in the parameter space, within the operational limits of the pumps, feeders and overall equipment performance. A central composite face-centered Design of Experiments (DoE) with three center points was performed for each granulator studied. Resulting granules were characterized by measuring their size distribution and porosity. Also, tensile strength and dissolution rate of tablets, made with them at same relative density, was assessed. For the specific study of granules size, the presence of fines and large granules was quantified to assess the process yield (in this work, granules between 125 and 2000 μm). For each response, a fitting equation considering all statistically significant parameters and their interactions, was obtained.

2. Materials

Ibuprofen 50 (BASF, Germany), lactose (Pharmatose 200M, DFE pharma, USA), microcrystalline cellulose (MCC, Avicel PH-101 NF, Dupont, USA), polyvinylpyrrolidone (PVP) average M.W. 50000 (K30, Acros Organics, USA), sodium hydroxide (VWR, USA), potassium phosphate (VWR, USA), croscarmellose sodium (CCS, Spectrum Chemical MFG, US) and distilled water were used.

3. Methods

3.1. Preparation of powder mixtures

Drug and excipients were blended in a 4-liters V-blender (Patterson Kelley, USA) for 30 minutes at 25 rpm. An intensifier bar (522 rpm) was used during mixing to improve powder dispersion movement. Powder batch size was kept constant (3 kg) to ensure the same blending conditions. Unlike previous investigations, this work considers a high drug loading (ibuprofen concentration in blend was theoretically fixed to 60% W%), limiting the quantity of fillers/excipients that can be added [15][16]. PVP was used as binder in a 3% W%. MCC and lactose were incorporated as granulation excipients, fixing the lactose to MCC ratio (lactose:MCC) at 70:30.

3.2. Drug quantification

Drug quantification in blends was assessed by UV-visible spectrophotometry (Agilent Cary 60 Spectrophotometer, Malaysia) in buffer phosphate pH 7.2 at 220 nm, according to USP44-NF39 ibuprofen chapter [17]. A stock solution of 1.25 mg/mL drug in buffer phosphate pH 7.2 was prepared and adequate dilutions were subsequently obtained. Linearity was demonstrated in the 0.0025-0.0200 mg/mL range. Blends were stored on plastic hermetic bags. Aliquots of the mixture were extracted from the upper, middle and lower strata of the storage bag for drug quantification.

3.3. Twin screw granulation (TSG)

Two twin screw granulators specifically suited for pharmaceutical applications were employed in this work: a Pharma 11 (Ph 11) granulator from ThermoFisher Scientific (Germany) and a QbCon system from L.B. Bohle (Germany). The QbCon system incorporates the drying chamber of QbCon 1 and the barrel dimensions of QbCon 25 [18], and for simplicity it will be referred to as QbCon throughout this work.

Characteristic dimensions of twin-screw granulators used for granule production are shown in Table 1. A short screw configuration was assembled for Ph 11. In this system, a kneading zone (KZ) of 60° was placed immediately after the liquid feed port. A second KZ of 30° was built and separated from the first KZ using conveying elements (14 pitch). A chopper was put at almost the end of the screw to reduce oversized granules. Wet granulation experiments on Ph 11 were carried out maintaining the temperature of the barrel jacket at 20 °C by a cooler/chiller (ThermoFisher Scientific, Germany). A gravimetric feeder (K-SFS-24, Coperion KTron, Inc., USA) was used to feed the powder into the system and granulation liquid was fed via a peristaltic pump (MasterFlex, Cole Parmer, USA).

Table 1. Dimensions of the two screw granulators

	D_0 [mm]	D [mm]	c_i [mm]	T [mm]	L_u /D [—]
Ph 11	11.0	10.7	0.15	2.38	25.75
QbCon	25.5	25.0	0.25	4.20	20.00

D_0: barrel diameter; D: screw diameter; c_i: screw to barrel clearance; T: trough; L_u/D: length to diameter ratio used in this work.

For the QbCon, the entire barrel length was used and screw configuration was kept constant and as similar as possible to the Ph 11, taking into account the different dimensions of the granulators. In this case, first KZ had a stagger angle of 67.5° and second KZ a straggled angle of 22.5°. Pitch between KZ was 14 and a chopper was put at the end of the screw. QbCon is a fully integrated system that includes the feeding of powder by a gravimetric feeder suitable for throughputs of 1–2.5 kg/h, the feeding of the liquid via a high-pressure pump, wet granulation and drying. The temperature was held constant at 20 °C by a cooler.

All experiments were run for 2 minutes to achieve stable conditions and for 10 minutes (if possible) to collect granules for characterization. Granules produced with both systems were air-dried in alumina pans at room temperature until their moisture content was similar to that in the original blend, *i.e.*, less than 2% W%, which typically required approximately 24 hours. Samples were stored on plastic hermetic bags and saved for analysis.

3.4. Design of experiments

First, an exhaustive screening process with 42 different parameters combinations was performed in the Ph 11 equipment to determine the functional range for LSR, N and TP (data not shown). Then, a central composite, face-centered DoE with three center points was developed. To enable a direct comparison, an analogous DoE with the same range for LSR was developed for the QbCon equipment. In this later case, the TP range is wider than for Ph 11 (but it contains it) and the N range was selected to obtain the same shear rate.

The LSR range was in agreement with previous studies [15][19]. Considering the hydrophobic nature of ibuprofen, LSR is expected to significantly impact granule characteristics. Highly hydrophobic blends are known to be susceptible to wetting issues and may necessitate higher LSR values [20]. On the other hand, ibuprofen has a relatively low melting point [16], making the drying process challenging as a high proportion of liquid must be removed at low temperatures. Consequently, the final LSR range was selected to effectively facilitate granule

formation while minimizing the liquid content to optimize the subsequent drying process. The selected LSR range was validated at both the highest and lowest levels.

Screw speed in the Ph 11 was first tested over a broad range (150-700 rpm), with the final range (250-450 rpm) determined by the feasibility of producing granules without physical impairment. As mentioned before, the corresponding screw speed for the QbCon system was selected to obtain similar shear rates in both systems,

$$\dot{\gamma}_r = \pi ND/(60c_i), \qquad \text{Eq. (1)},$$

where the screw speed N is given in rpm, D is the screw diameter and c_i is the screw to barrel clearance (see Table 1). Following Zhang et al., the characteristic value of the shear rate field acting on the material was calculated in the overflight gap [5]. The formulation and LSR were kept the same for both systems, suggesting that the rheological behavior of the material would also be similar in both granulators. Additionally, the screw configuration and L/D were also similar between the two systems. As a result, a similar shear stress field is expected in both granulators.

Throughput in the Ph 11 was chosen to be compatible with the gravimetric feeder coupled to the granulator after calibrating the feeder with the blend.

Powder feed number, PFN, is defined as

$$\text{PFN}=\frac{\text{TP}}{\rho_b \omega D_0^3}, \qquad \text{Eq. (2)},$$

where TP is the mass flow rate of the powder, ρ_b is the bulk density of the powder, ω is the angular velocity of the shaft and D_0 is the barrel diameter [11], and can be used as a scale parameter. Due to mechanical limitations of the granulators, it was not possible to achieve the same PFN in both systems. Therefore, in this work only the shear rate was used as the constant parameter to assess process transferability between systems.

Each DoE was generated and evaluated using Statgraphics® Centurion version XV software (Statpoint Technologies Inc., USA). A total number of 17 runs were performed for each system in a randomized order. A summary of the design matrix and the level of each variable used are shown in Table 2 while in Table S1 (supplementary material) can be seen the whole DoE design for QbCon and Ph 11 granulators. Software was used to find suitable fitting models from the general following Equation 3:

$$Y=b_0+\sum_{i=1}^{3} b_i x_i + \sum_{i=1}^{2}\sum_{j>i}^{3} b_{ij} x_i x_j + \sum_{i=1}^{3} b_{ii} x_i^2 \qquad \text{Eq. (3)}$$

where Y is the response studied; b_0 is the intercept; b_i, b_{ij} and b_{ii} are the main effect coefficient, interaction between two factors coefficient and quadratic effect coefficient, respectively; and x_i and x_j are the considered factors (i and j range from 1 to 3).

Table 2. Levels of independent variables

	Ph 11			**QbCon**		
	LEVELS			LEVELS		
FACTORS	-1	0	1	-1	0	1
LSR	0.2	0.3	0.4	0.2	0.3	0.4
TP (Kg/h)	0.7	0.9	1.1	0.7	1.2	1.7
N (rpm)	250	350	450	180	250	320
$\dot{\gamma}_r$ (s^{-1})	934	1307	1681	942	1309	1676

Coefficients were calculated considering the experimental responses. Analysis of variance (ANOVA) was used to determine the statistical significance of studied factors and their interactions on the responses obtained. Model terms with *p*-values lower than 0.05 were considered statistically significant and non-significant terms were deleted from the particular equation for a given response except when they increased the quality of the fit or for hierarchy principle (which indicates that all the main effects of significant higher-order terms or interactions must be kept, even if the main effect *p*-value is larger). The regression model adequacy was evaluated by the statistical coefficient R^2.

3.5. Sieving between 125-2000 μm

Granules obtained were sieved for 10 min using amplitude of 4 mm, through 125 and 2000 μm sieves (Octagon sieve shaker, Endecotts Ltd., UK). Here, fine granules (W_F) were defined as those with size smaller than 125 μm while over-granulated material or lumps (W_L) was considered for granules with size larger than 2000 μm. The fraction of granules with size between 125-2000 μm was considered the yield of the granulation process, considering that over- or under-granulated material can impact flowability, drying time, tablet mass uniformity and/or segregation during compression and content variation, among others [21][22]. Cut off diameters were selected based on bibliography [23][24]. Unless otherwise stated, only the 125-2000 μm fraction was used for further characterization.

3.6. Granule drug composition

Drug content in granules from both DoE was assessed in the same way as drug composition was studied in blends. Samples of the granules were taken from the top, middle and bottom of the bag where they were stored.

3.7. Granule size distribution

Granule size distribution (GSD) of sieved granules was measured using the Eyecon (Innopharma Laboratories, Ireland) particle imager. A representative sample from different points of the storage bag was collected from each DoE run for both granulators and placed on a dish. Results of GSD parameters are average of four to eight samples from which 25 pictures were taken and processed by Eyecon software.

Span value, as indicative of the spread of the GSD, was calculated for each DoE run as showed in Equation 4:

$$\text{Span} = \frac{(D_{90} - D_{10})}{D_{50}}, \qquad \text{Eq. (4)},$$

where D_{10}, D_{50} and D_{90} represent the diameters below which 10%, 50% and 90%, by volume, of the granule population lies, respectively.

3.8. Envelope density

The envelope density of the granules was assessed in a Geopyc 1360 (Micromeritics, USA) with DryFlo™ as solid medium. The system gives reliable results for particles larger than 1000 μm, thus, granules obtained from each experiment were first sieved to separate the 1000-2000 μm fraction. Results are the average of four experiments.

3.9. True density

The true density of granules with 1000-2000 μm was studied in a helium pycnometer (AccuPyc II 1340, Micromeritics, USA). Porosity was calculated using the true and envelope density [25], as shown in Equation 5:

$$\varepsilon = 1 - \frac{\rho_e}{\rho_t}, \quad \text{Eq. (5)}$$

where ρ_e and ρ_t are the envelope and true densities, respectively.

3.10. Maximum saturation level calculations

The maximum liquid saturation level for each DoE run at both system were calculated as previously described [26], using Equation 6

$$S_{max} = w\rho \frac{1-\varepsilon_{min}}{\varepsilon_{min}}, \quad \text{Eq. (6),}$$

where ρ is the particles to liquid density ratio, w is the mass ratio of liquid to solid, and ε_{min} is the minimum porosity for a particular set of operating conditions. In this work, granule porosity calculated using Eq. 6 was considered the ε_{min} that granules can reach after a given lapse of residence time for a continuous process [27].

3.11. Tablet production

Approximately 333 mg of granules in the 125-2000 μm range (carrying *ca*. 200 mg of ibuprofen) were compacted in a manual press (One Tablet Press, Adamus, Poland) using a die of 10 mm. Granules were manually feed into the die (filling depth of *ca*. 10-14 mm). Force was selected for each DoE run (7.4-8.9 KN) in order to obtain tablets with same relative density (0.91). Additionally, a separate set of tablets incorporating 3% W% CCS were produced under identical conditions and stored for subsequent dissolution testing.

3.12. Tablet tensile strength

Tablet hardness, F, expressed in newton [N], tablet thickness, h, and tablet diameter, D, in millimeters [mm] were measured using a Pharmatron MultiTest 50 hardness tester (Pharmatron, Switzerland). Tablet tensile strength, σ, in MPa, was calculated using Equation 7 [28]:

$$\sigma = \frac{2F}{\pi Dh}, \quad \text{Eq. (7)}$$

3.13. Dissolution

Dissolution of tablets was studied using a USP apparatus 2 (Agilent, Malaysia), coupled to an automatic Dissolution Sampling Station (Agilent 8000, Malaysia) and UV-visible. Dissolution medium was buffer phosphate pH 7.2. Paddle rpm was set at 50 and medium temperature was kept at 37 °C. Samples were withdrawn every 5 minutes, read in-line and returned to the vessels. Results are the average of three experiments.

4. Results

In this work, we compare properties of granules obtained from two granulators of different scales but with similar screw configurations to study the process transferability under certain process conditions, without an explicit goal to increase the throughput of the process.

4.1. Content uniformity

Content uniformity was initially tested as a function of granule size. Similar results were obtained for fractions > 125 μm, 125-2000 μm and < 2000 μm (data not shown).

Within each DoE, content uniformity of sieved granules across all runs is within the variability of ibuprofen content determined in the blend (58±2% W%, in close agreement with the nominal drug content in the blend (60% W%), see Figure S2 in Supplementary material). No

statistically significant differences were observed between the mean of each system and the blend (Ph 11, *p*-value = 0.7; QbCon, *p*-value = 0.7) nor between all runs in both systems (*p*-value = 0.8). Specifically, drug content was 57±2% W% for granules in both systems, as shown in Figure S2.

4.2. Granule size distribution

The granule size distribution (GSD) was characterized by determining D_{50} of the sieved sample. In Figure 1a, D_{50} is presented as a function of LSR. In Figure 1b, D_{50} is nondimensionalized by the maximum screw clearance, gap or screw trough (the maximum clearance between the screw flights and the inner surface of the barrel), T= 2.38 mm and 4.20 mm for Ph 11 and QbCon, respectively (see Table 1). Granule size distributions were mostly monomodal in all cases, as shown in Figure S3 (supplementary material).

Although D_{50} values increase with LSR for both systems, they present different dependence. The Ph 11 showed little change for LSR values less than 0.3 but exhibited a drastic increase at an LSR of 0.4. In contrast, the QbCon displayed a steady increase in D_{50} as a function of LSR.

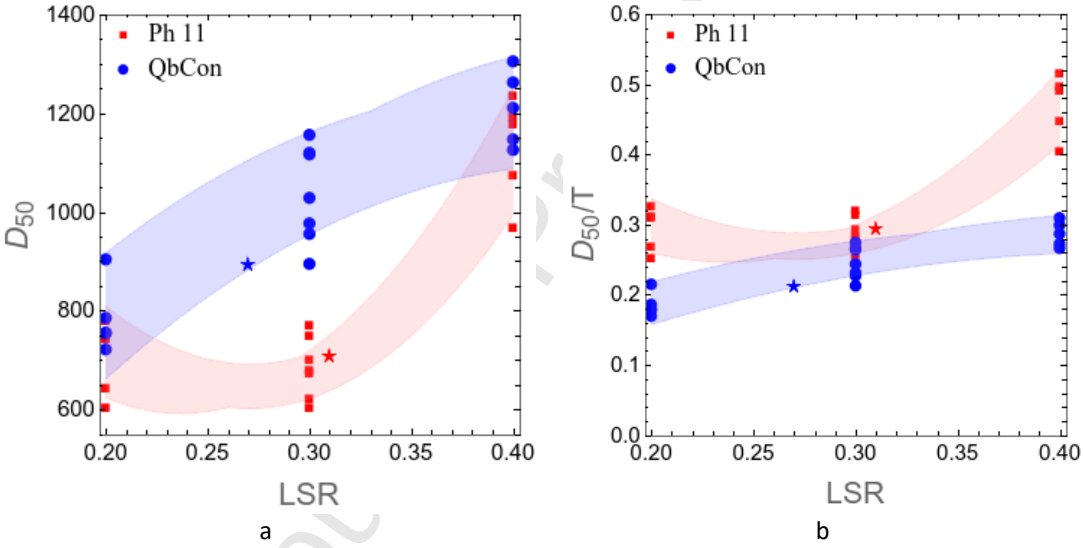

a b

Figure 1: a) D_{50} dependance with LSR. The red squares represent the Ph 11, while the blue circles the QbCon. The shadow areas correspond to the regions where the best fitted equation would exist. The fitting equation is a hyper-surface that, when projected into the 2D graph of Figure 1, corresponds to the region represented by the shadow area. It is worth noting that the shaded area is not a confidence interval, but with no clear dependance of its variation with other parameters, it might be taken as the D_{50} variability. b) D_{50} normalized as a function of trough (T) size (2.38 mm for Ph11 and 4.20 mm for QbCon).

It was observed that D_{50} shows a stronger dependence on the LSR compared to other parameters. Therefore, Figure 1 illustrates only this dependence and the effect of the other parameters is represented by the shaded areas in this figure. Specifically, the shaded area corresponds to the projection of hyper-surface that best fits D_{50} as a function of all the parameters onto the LSR axis. It is important to note that these shaded regions are not confidence intervals; however, without clear dependence on other parameters, it may be interpreted as the variability of the response (in this case D_{50}). The actual response surface plots of D_{50} as a function of LSR and N, with TP fixed at the center level, are presented in the supplementary material (Figure S4a and Figure S4b). ANOVA analysis, also shown in the

supplementary material, confirms that LSR has the largest effect on D_{50}, including linear and quadratic terms. Smaller contributions from interactions between LSR and N were seen for both systems. Also, N^2 contribution was significant for QbCon. Supplementary material includes fitting equations for both systems along with R^2 values in Table S2 and Table S3. It is worth noting the interaction at high LSR in the Ph 11 system, where an increase in N results in a decrease in D_{50}, a trend not observed at lower LSR values. Finally, the adjusted R^2 for the D_{50} response is 94.6 and 91.7 for Ph 11 and QbCon, respectively.

Also, D_{50} was nondimensionalized using the screw trough as the characteristic length scale of the equipment, but the analysis of the results does not vary much when other length scales are used (e. g. the barrel diameter or the minimum gap in the kneading zones, data not shown) given that their ratio between the two systems is similar, ranging between 2.50 and 2.35. The dimensionless D_{50}/T shown in Figure 1b agrees in both systems for the intermediate LSR=0.3 but are clearly different for LSR=0.4. Notably, the Ph 11 demonstrates larger dimensionless granule sizes and a more pronounced size increase between LSRs of 0.3 and 0.4 compared to the QbCon.

The size distribution of granules was also characterized by the span value, as defined in Eq. (4). Like D_{50}, the most significant dependence occurs with LSR. Figure 2 shows the decrease of span values with increasing levels of LSR for both systems. This figure also presents the range of the model equations considering the dependence on all the parameters. Particularly, besides the linear and quadratic influence of LSR, the N^2 (for both systems) and the interaction between N and LSR (only for Ph 11) contributions demonstrated to be statistically significant. The adjusted R^2 value for this response is relatively low for the Ph 11 (59.8) but higher for the QbCon (90.0), indicating a better fitting for the latter. The response surfaces are presented in the supplementary material in Figure S5 along with the fitting equations (Table S2 and Table S3).

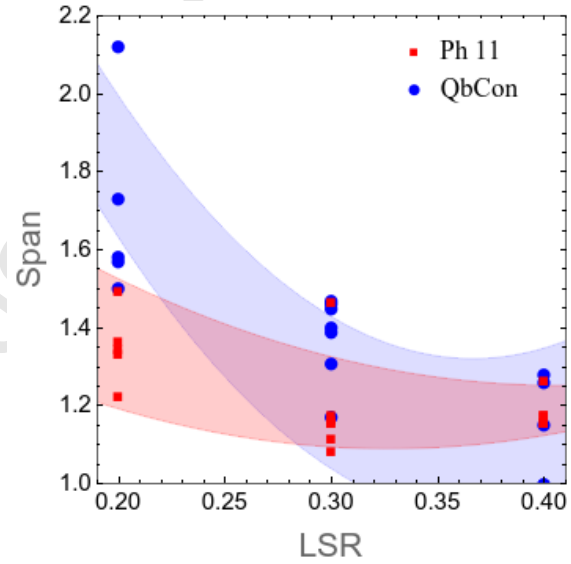

Figure 2: Span dependence with LSR. The red squares and blue circles correspond to the Ph 11and QbCon, respectively. The shadow areas relate to the regions where the fitted equations exist. The corresponding equations are given in the supplementary material.

The increasing values of D_{50} with LSR observed in Figure 1 for both systems suggest that small values of LSR would result in a significant number of fines and larger values of LSR could produce a large fraction of over-granulated material or lumps. This behavior is in fact observed for both systems, as shown in Figure 3, where the fraction of fines (W_F) decreases with LSR and the fraction of over-granulated material (W_L) increases with LSR.

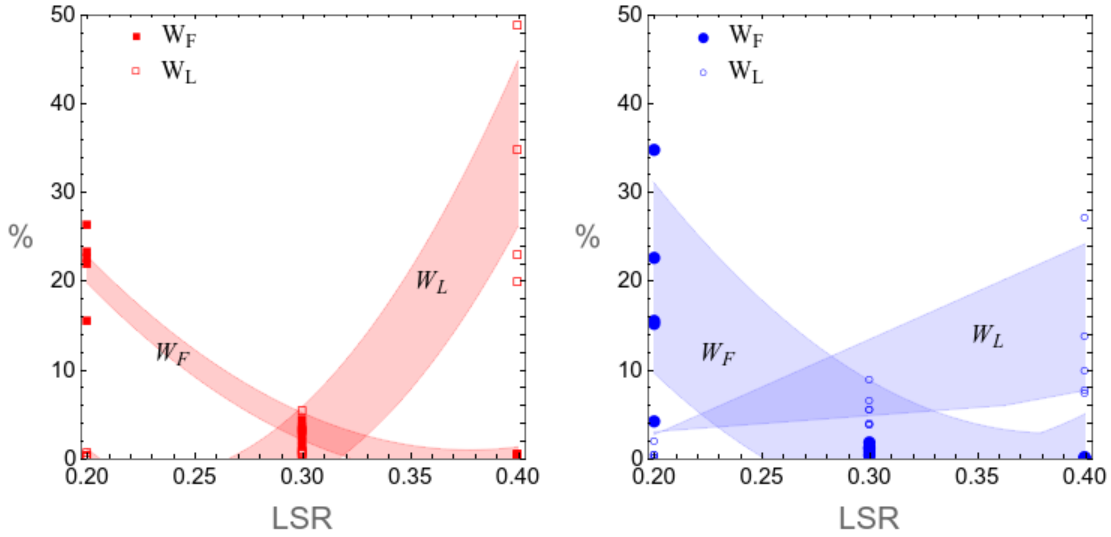

Figure 3: Fraction of fines and over-granulated material a) Ph 11 and b) QbCon. The shaded areas correspond to the range of the model fitting equations reported in the supplementary material.

The fraction of fines and large granules exhibits a strong dependence on LSR and, as it can be seen, the dependence of the production of over-granulated material in the QbCon is linear with LSR, while it is quadratic for the other cases. Also, a weaker dependence on other process parameters and their interactions was found. In fact, N and the interaction between LSR and N were statistically significant for the production of over-granulated material in both systems. Additionally, TP was shown to be significant for the production of fines in the QbCon but not in the Ph 11.

The estimated response surfaces, fitting equations and corresponding R^2 values are presented in the supplementary material in Figure S6 and Table S2 and Table S3. As before, their projection into the 2D graph is represented by the shaded areas. For the Ph 11 system, the models for fines and lumps have adjusted R^2 values of 96.1 and 88.1, respectively. In the QbCon, these values are 80.2 and 82.0, respectively.

4.3. Porosity

In Figure 4, the porosity of the sieved granules is presented as a function of LSR for both granulators. An unexpected initial increase in porosity with LSR is observed in the Ph 11. On the other hand, the QbCon shows an almost constant porosity when LSR increases from 0.2 to 0.3. In both systems there is a significant decrease in porosity when LSR further increases to 0.4. As a result, the quadratic LSR term was the most significant for the Ph 11 but the linear term was more significant to describe the porosity in the QbCon. TP and N were statistically significant for the analysis, either directly or through interactions. The response surfaces are presented in the supplementary material in Figure S7 together with the fitting equations and the statistically relevant processes parameters and corresponding interactions in Table S2 and Table S3. The dependence with the other parameters is not as significant as the one with LSR and it is represented by the shadow areas in Figure 4. The adjusted R^2 values for this response in Ph 11 and QbCon are 90.3 and 92.7, respectively.

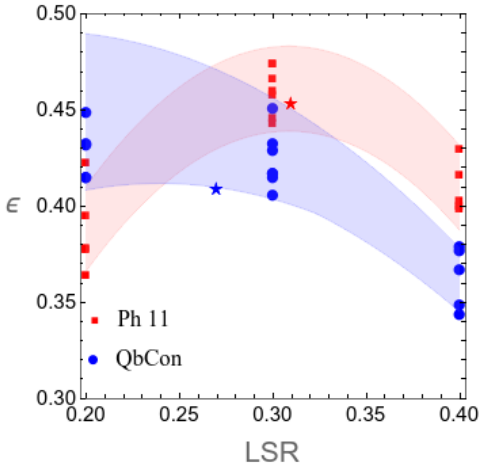

Figure 4: Porosity ε as function of LSR, red squares and blue circles correspond to the Ph 11 and QbCon, respectively. The shadows areas correspond to the region where the fitted equations exist.

4.4. Compaction

Tablets, the intended final pharmaceutical form, were obtained by compacting granules. For adequate handling during manufacturing, packaging and patients use, tablets should have sufficient mechanical strength, usually measured by the tensile strength [29]. Tablets with tensile strength of at least 2 MPa typically enable further processing as well as transport [30]. Therefore, tensile strength was measured for tablets made with granules of all DoE runs in both systems and compacted to a relative density of 0.91.

Although the sieved granules had different critical quality attributes, the resulting tablets exhibited similar behavior. It is worth noting that all DoE runs led to tablets above the threshold tensile strength value of 2 MPa.

The two critical attributes studied for the produced granules, that is GSD and porosity, did not show a significant impact on the tablet tensile strength, independent of the system used. Figure 5a and Figure 5b show the tablet tensile strength as a function of D_{50} and porosity, respectively. The measured tensile strength is slightly larger for the tablets obtained with granules from the QbCon system compared to those obtained with Ph 11, even though the porosity of QbCon granules is smaller than those obtained with Ph 11. For reference, the tensile strength measured for tablets obtained by compacting the blend under the same conditions is included in Figure 5. As it can be seen, the tensile strength is markedly higher for tablets obtained by compacting granules, as previously reported [31].

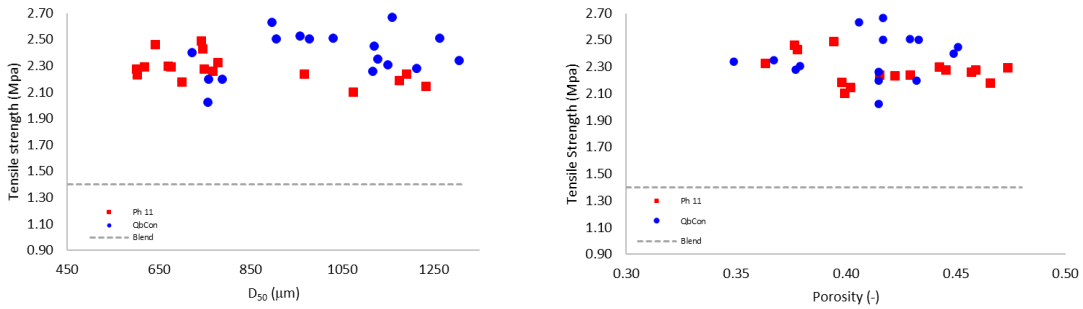

a b

Figure 5. Relationship between each DoE responses and tablet tensile strength. a) tensile strength as a function of D_{50}. b) tensile strength as a function of porosity.

4.5. Dissolution

Dissolution testing was conducted on tablets formulated across the LSR range (0.2, 0.3 and 0.4) for both equipment. Dissolution profiles are presented in Figure S8 (supplementary material) Although Ibuprofen is classified as a Class II drug in the Biopharmaceutics Classification System (BCS), characterized by low solubility and high permeability [32], all tested tablets met the dissolution criteria specified in the USP monograph [33]. This monograph mandates that ibuprofen tablets should release at least 80% of the active ingredient within 60 minutes. Notably, all samples achieved approximately 80% ibuprofen dissolution within approximately 20 minutes

5. Discussion

One of the main goals of granulation is to achieve uniform product content, a critical quality attribute. In this work, granules produced in all DoE runs demonstrated uniform ibuprofen content, independent of process parameters and closely aligned with the content in the blend determined in independent experiments. Given the hydrophobicity of the ibuprofen and its presence of more than 50% W% in the formulation, achieving content uniformity across all DoE runs is a positive outcome. This consistent content uniformity is reflected in the dissolution profiles of tablets, regardless the LSR level tested. These profiles demonstrated consistent drug release, meeting the criteria outlined in the USP monograph for both granulation systems evaluated. Additionally, even though the size and porosity of the granules varied considerably with LSR and with the system employed, no significant difference in tensile strength is observed in the tablets manufactured from the different granules.

ANOVA analysis revealed that LSR was the most significant factor influencing granule size, subsequently impacting the mass of fines and lumps. This finding agrees with previous research [6][11][34][35][36][37][38]. As expected, increased liquid content within the system leads to enhanced granule growth. Within the kneading zones, liquid is expelled from the granule interior towards the surface, facilitating the layering of unwetted particles. Concurrently, in the conveying regions, capillary forces between granules promote coalescence [26]. A comprehensive investigation into the intricate mechanisms by which LSR influences wetting behavior, granule nucleation and growth are beyond the scope of this study. In general terms, smaller D_{50} and W_F but higher W_L values were obtained for the Ph 11 system when directly compared to the QbCon. The smaller D_{50} values in this system are somewhat expected considering the smaller gap size in this equipment [39]. Additionally, almost negligible W_L values were obtained for LSR of 0.2 and 0.3, but at an LSR of 0.4, the W_L values increased significantly which was an unexpected result. On the other hand, higher W_L at LSR of 0.3 was observed for QbCon compared to Ph 11. However, W_L was not as prominent when LSR was 0.4 in the QbCon compared to the Ph 11.

As shown in Figure 1a, D_{50} differs significantly at an LSR of 0.3, with the QbCon producing granules approximately 35% larger than the Ph 11. While variations in D_{50} are expected due to differing equipment dimensions, normalizing D_{50} by a characteristic length (e.g., the trough) should yield similar values if process parameters were successfully transferred from one granulator to the other. This is not the case in general for our systems as an overlap in normalized granule size is only seen at LSR=0.3 (see Figure 1b). Osorio et al found that the dimensions of the barrel (between 11 and 24 mm) have a larger impact on the granule size increase than LSR (varied between 0.15 and 0.3 in their case) for their formulation consisting mainly of lactose and microcrystalline cellulose [11]. However, we found the opposite behavior:

the impact of LSR is much larger than the impact of the diameter of the barrel. These disparities reveal the complexity of the granule formation process.

Considering all DoE runs in both systems, up to 35 and 50% of granules fell outside the size specification range (125-2000 µm) when LSR was set at 0.2 or 0.4, respectively. This is illustrated in Figure 6, where the yield, defined as the fraction of granules within the 125-2000 µm size range, is plotted against the LSR.

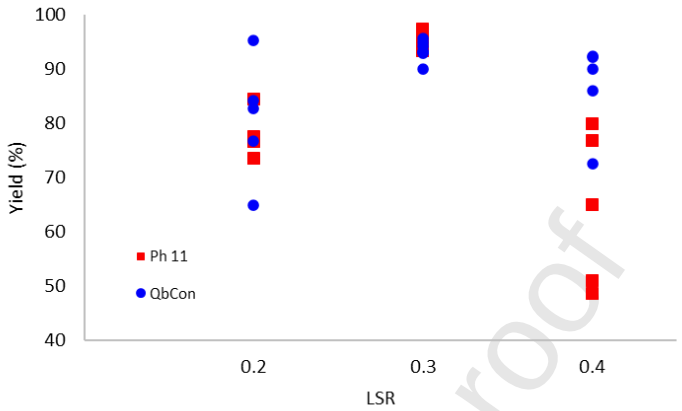

Figure 6. Yield (%, fraction of granules within the 125-2000 µm size range) vs. LSR for both granulators.

Importantly, process yield is almost the same for both systems at LSR=0.3 (around 90% and higher). The recommendation for the present formulation is then to work around LSR=0.3. This is highlighted with star points in Figure 1 and Figure 4, and will be further discussed later when optimization is presented.

Considering a fully continuous process where the sieving step used in this work cannot be performed, the granule yield becomes critical. Having granules outside size specifications can impact downstream processes such as drying, transport and dosing, as well as the final product properties, including tablet friability and content uniformity. In fact, high quantities of oversized granules lead to longer drying times and large lumps can retain moisture in the core even if the external surface appears dry, potentially causing stability issues. Conversely, ungranulated material or very small granules can decrease flow properties, induce segregation and hinder content uniformity in the final product [22][40][41][42][43][44].

Besides the mean granule size, another useful metric related to the size distribution of the granules is the width of the distribution, characterized by the span value. A relatively narrow GSD is desirable as it ensures a uniform drying pattern across the granule population [6], which is particularly relevant for continuous processes where drying times are typically short [45]. Span values below 3 have been proposed as acceptable for a wet TSG [21]. Interestingly, the span value is similar when the LSR is 0.4 in both systems, but this response differs significantly at low and moderate LSR values. In this work, mostly monomodal granule size distributions were obtained for all DoE runs in both systems, as can be seen in Figure S3 (supplementary material). The granule size distribution narrowed when LSR increased (as can be seen from span values in Figure 2), which agrees with previous work [6][25][46]. This trend is more pronounced in the QbCon than in the Ph 11.

Another relevant response is the granules porosity (ε), as it affects tabletability, tablet friability and density, which in turn impacts downstream processes [23]. The observed decrease in ε as LSR increased from 0.3 to 0.4 (Figure 4) could be expected, as additional liquid at the granule surfaces would promote strong densification and consolidation due to the plastic behavior of

the granules [6][47][48]. However, this behavior was not observed when LSR increased from 0.2 to 0.3. The increase in porosity for the Ph 11 system and the nearly constant porosity for the QbCon when LSR increases from 0.2 to 0.3 could be attributed to the fact that LSR=0.2 may only allow a small extent of granulation [49]. This correlates very well with the high amount of fines quantified at this LSR.

In order to get a better insight into the granulation process, it is useful to consider the maximum granule pore saturation, S_{max}, (see Eq. (6)) which depends on both LSR and porosity and is indicative of the liquid content on granules needed for granulation. When no liquid is available on the surface of the granules (due to low LSR or large porosity), the granule growth mechanism based on capillary-bridge formation stops, thus determining the granule size. Therefore, an increase in S_{max} would in principle predict an increase in granule size (as well as a decrease in the amount of fines and an increase in the number of lumps) [11][50][51][52][53]. D_{50}/T as a function of S_{max} presents a monotonic growth for both Ph 11 and QbCon, as shown in Figure 7.

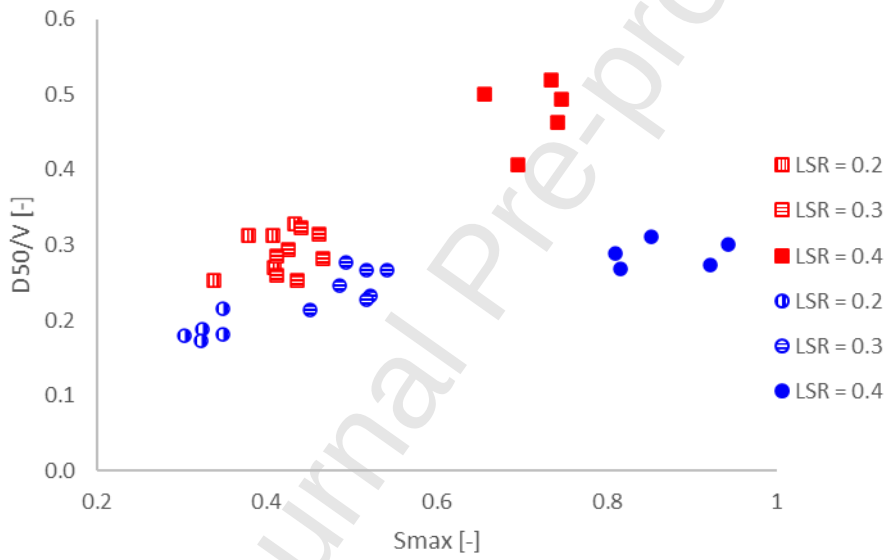

Figure 7: D_{50}/T as function of S_{max}. Red squares represent the Ph 11 while blue circles represent the QbCon. Different fillings indicate the three different LSR levels.

We performed an optimization exercise, with the goal of minimizing the production of fines and lumps while maximizing porosity. The three considered responses for optimization were assigned equal weight in the desirability function and had the same impact.

The optimum values for the process parameters were determined to be N=402 RPM and TP=1 Kg/h in the Ph 11. It is worth noticing that, as the range of maximum and minimum granule sizes is kept the same for both granulators, and the QbCon produces larger granules than the Ph 11, the optimum values obtained may lean towards different ranges in the parametric space, where the granule size tends towards lower values for the QbCon and larger for the Ph 11. As a result, for the Ph 11 system, the optimal values for N and TP are close to the maximum levels tested. For the QbCon, the optimal value for TP is the lowest value tested in the design of experiments (0.7 kg/h) and N was determined to be 264 RPM. In both cases, the optimal LSR value was found to be around 0.3, with a lower value for the QbCon (0.27) and a larger for the Ph 11 (0.31). The corresponding values of the response variables are shown with star symbols in Figure 1 and Figure 4. It needs to be considered that D_{50} response was not optimized; rather,

the corresponding D_{50} values were obtained through maximizing porosity and minimizing unusable granules.

The optimal LSR values are striking, especially considering the hydrophobic nature of the granulated active ingredient. Higher LSR have been reported for drugs with limited wettability [21]. This suggests that the excipients chosen for the granulation process, together with the selected screw speed and throughput used in the granulators, enables the production of granules with adequate critical attributes at relatively low LSRs.

It is worth noting that a screw speed of 402 RPM in the Ph 11 system corresponds to a shear rate of 1501 s^{-1}, while 264 RPM in the QbCon system corresponds to a shear rate of 1382 s^{-1}, indicating less than a 10% difference between granulators. Notably, at a LSR of 0.3, the granules differ significantly between the systems in terms of D_{50}, a critical response, but have a similar dimensionless D_{50}/T. Specifically, QbCon granules are approximately 35% larger than those obtained with Ph 11 for a LSR of 0.3. This difference is between 7 and 11% at LSR of 0.4 and 0.2, respectively. This analysis shows that the aim of comparing granules obtained at the same shear rate (and not screw speed) for the two different systems was more relevant [54]. The dimensionless granules size presents the same value for both equipment for LSR=0.3 (see Figure 1b), which corresponds to a close value to the optimum configuration.

6. Conclusions

In this study, two different granulators were used to produce granules with a high concentration of ibuprofen. The LSR emerged as the most influential factor affecting all responses examined across all DoE runs. Granules were obtained with a consistent content of ibuprofen that agrees with its bulk content in the blend. QbCon displayed lower porosity than the Ph 11 and the lowest porosity values were found at the highest LSR value, as anticipated. In general terms, the Ph 11 system exhibited smaller D_{50} values compared to the QbCon, as expected from their barrel diameter, but the scaling factor depends on LSR. Granule size distribution narrowed with increasing LSR in the QbCon, while the Ph 11 system displayed no clear trend. Process yield was similar across both systems at an LSR of 0.3, despite significant differences between systems at LSR values of 0.2 and 0.4.

Based on the comparative analysis performed in this work, it can be concluded that maintaining the same geometry and shear rate is not sufficient for a direct transfer of the granulation process from one system to another. This reveals the complexity of the granule production in a twin screw granulator, as the shear stress fields are expected to be similar but the granules exhibit different characteristics. However, it is possible to achieve granules with either identical or highly similar properties by adjusting process parameters within the operating range of granulators with different dimensions. Another important result is that despite differences in granule properties between both systems, the granules produced exhibited similar tensile strengths in tablet form, indicating the robustness of the formulation in final product properties. Also, similar dissolution profiles were obtained for all LSR in both systems.

Acknowledgments

N. Ceschan, MC. Balbi and P. Ravazzoli thank CSOPs for their technical assistance and hosting.

Funding

MinCyT (Prácticas de formación académica y profesional en el exterior para argentinos/as, Res. RESOL-2022-572-APN-MCT), Universidad Nacional del Sur (Res. CSU-647, Expte. 3068/22)

References

[1] S.L. Lee, T.F. O'Connor, X. Yang, C.N. Cruz, S. Chatterjee, R.D. Madurawe, C.M.V. Moore, L.X. Yu, J. Woodcock, Modernizing Pharmaceutical Manufacturing: from Batch to Continuous Production, J. Pharm. Innov. 10 (2015) 191–199. https://doi.org/10.1007/s12247-015-9215-8.

[2] M. Ierapetritou, F. Muzzio, G. Reklaitis, Perspectives on the Continuous Manufacturing of Powder-Based Pharmaceutical Processes, Am. Inst. Chem. Eng. J. 62 (2016) 1846–1862. https://doi.org/10.1002/aic.

[3] S. Sacher, J.. Khinast, An Overview of Pharmaceutical Manufacturing for Solid Dosage Forms, in: R. Ierapetritou, M.G., Ramachandran (Ed.), Process Simul. Data Model. Solid Oral Drug Dev. Manuf. Methods Pharmacol. Toxicol., Humana, New York, NY, New York, 2016. https://doi.org/https://doi.org/10.1007/978-1-4939-2996-2_10.

[4] P. Suresh, I. Sreedhar, R. Vaidhiswaran, A. Venugopal, A comprehensive review on process and engineering aspects of pharmaceutical wet granulation, Chem. Eng. J. 328 (2017) 785–815. https://doi.org/10.1016/j.cej.2017.07.091.

[5] Y. Zhang, T. Liu, S. Kashani-Rahimi, F. Zhang, A review of twin screw wet granulation mechanisms in relation to granule attributes, Drug Dev. Ind. Pharm. 47 (2021) 349–360. https://doi.org/10.1080/03639045.2021.1879844.

[6] M. Verstraeten, D. Van Hauwermeiren, K. Lee, N. Turnbull, D. Wilsdon, M. am Ende, P. Doshi, C. Vervaet, D. Brouckaert, S.T. Mortier, I. Nopens, T. De Beer, In-depth experimental analysis of pharmaceutical twin-screw wet granulation in view of detailed process understanding, Int. J. Pharm. 529 (2017) 678–693. https://doi.org/10.1016/j.ijpharm.2017.07.045.

[7] M. Wu, D. Sun, T. Zhang, C. Zhou, B. Zhang, Study on the Function of Conveying, Kneading Block and Reversing Elements on the Mixing Efficiency and Dispersion Effect inside the Barrel of an Extruder with Numerical Simulation, Foods. 12 (2023). https://doi.org/10.3390/foods12183503.

[8] A. Schmidt, H. de Waard, P. Kleinebudde, M. Krumme, Continuous Single-Step Wet Granulation with Integrated in-Barrel-Drying, Pharm. Res. 35 (2018) 1–16. https://doi.org/10.1007/s11095-018-2451-0.

[9] S. Lute, R.M. Dhenge, A.D. Salman, Twin Screw Granulation: An Investigation of the Effect of Barrel Fill Level, Pharmaceutics. 10 (2018). https://doi.org/10.3390/pharmaceutics10020067.

[10] D. Djuric, B. Van Melkebeke, P. Kleinebudde, J.P. Remon, C. Vervaet, Comparison of two twin-screw extruders for continuous granulation, Eur. J. Pharm. Biopharm. 71 (2009) 155–160. https://doi.org/10.1016/j.ejpb.2008.06.033.

[11] J.G. Osorio, R. Sayin, A. V. Kalbag, J.D. Litster, L. Martinez-Marcos, D.A. Lamprou, G.W. Halbert, Scaling of Continuous Twin Screw Wet Granulation Juan, AIChE J. 63 (2016) 921–932. https://doi.org/10.1002/aic.

[12] A. Nastaj, K. Wilczyński, Optimization and scale-up for polymer extrusion, Polymers (Basel). 13 (2021). https://doi.org/10.3390/polym13101547.

[13] L. Kotamarthy, C. Sampat, R. Ramachandran, Development of a Granule Growth Regime Map for Twin Screw Wet Granulation Process via Data Imputation Techniques, Pharmaceutics. 14 (2022) 2211. https://doi.org/10.3390/pharmaceutics14102211.

[14] R. Meier, M. Thommes, N. Rasenack, K.P. Moll, M. Krumme, P. Kleinebudde, Granule size distributions after twin-screw granulation – Do not forget the feeding systems, Eur. J. Pharm. Biopharm. 106 (2016) 59–69. https://doi.org/10.1016/j.ejpb.2016.05.011.

[15] A. Schmidt, H. De Waard, K.P. Moll, M. Krumme, P. Kleinebudde, Quantitative assessment of mass flow boundaries in continuous twin-screw granulation, Chimia (Aarau). 70 (2016) 604–609. https://doi.org/10.2533/chimia.2016.604.

[16] J. Zhao, G. Tian, H. Qu, Application of I-Optimal Design for Modeling and Optimizing the Operational Parameters of Ibuprofen Granules in Continuous Twin-Screw Wet Granulation, Biomedicines. 11 (2023) 2030. https://doi.org/10.3390/biomedicines11072030.

[17] Ibuprofen, in: USP44-NF39, 2021.

[18] S. Pohl, Transfer of twin-screw granulation processes and predictions of barrel fill, Heinrich-Heine-Universität Düsseldorf, 2022.

[19] M. Maniruzzaman, A. Nair, M. Renault, U. Nandi, N. Scoutaris, R. Farnish, M.S.A. Bradley, M.J. Snowden, D. Douroumis, Continuous twin-screw granulation for enhancing the dissolution of poorly water soluble drug, Int. J. Pharm. 496 (2015) 52–62. https://doi.org/10.1016/j.ijpharm.2015.09.025.

[20] S. Kashani Rahimi, S. Paul, C.C. Sun, F. Zhang, The role of the screw profile on granular structure and mixing efficiency of a high-dose hydrophobic drug formulation during twin screw wet granulation, Int. J. Pharm. 575 (2020) 118958. https://doi.org/10.1016/j.ijpharm.2019.118958.

[21] F. Stauffer, V. Vanhoorne, G. Pilcer, P.F. Chavez, C. Vervaet, T. De Beer, Managing API raw material variability during continuous twin-screw wet granulation, Int. J. Pharm. 561 (2019) 265–273. https://doi.org/10.1016/j.ijpharm.2019.03.012.

[22] N. Willecke, A. Szepes, M. Wunderlich, J.P. Remon, C. Vervaet, T. De Beer, A novel approach to support formulation design on twin screw wet granulation technology: Understanding the impact of overarching excipient properties on drug product quality attributes, Int. J. Pharm. 545 (2018) 128–143. https://doi.org/10.1016/j.ijpharm.2018.04.017.

[23] D. Djuric, P. Kleinebudde, Impact of screw elements on continuous granulation with a twin-screw extruder, J. Pharm. Sci. 97 (2008) 4934–4942. https://doi.org/10.1002/jps.21339.

[24] Y. Liu, M.R. Thompson, K.P. O'Donnell, Function of upstream and downstream conveying elements in wet granulation processes within a twin screw extruder, Powder Technol. 284 (2015) 551–559. https://doi.org/10.1016/j.powtec.2015.07.011.

[25] W. Meng, K.S. Rao, R.D. Snee, R. Ramachandran, F.J. Muzzio, A comprehensive analysis and optimization of continuous twin-screw granulation processes via sequential experimentation strategy, Int. J. Pharm. 556 (2019) 349–362. https://doi.org/10.1016/j.ijpharm.2018.12.009.

[26] S.M. Iveson, J.D. Luster, Growth regime map for liquid-bound granules, AIChE J. 44 (1998) 1510–1518. https://doi.org/10.1002/aic.690440705.

[27] W. Meng, L. Kotamarthy, S. Panikar, M. Sen, S. Pradhan, M. Marc, J.D. Litster, F.J. Muzzio, R. Ramachandran, Statistical analysis and comparison of a continuous high shear granulator with a twin screw granulator: Effect of process parameters on critical granule attributes and granulation mechanisms, Int. J. Pharm. 513 (2016) 357–375. https://doi.org/10.1016/j.ijpharm.2016.09.041.

[28] J.T. Feel, J.M. Newton, Determination of Tablet Strength by the Diametral-Compression Test, J. Pharm. Sci. 59 (1970) 688–691. https://doi.org/doi.org/10.1002/jps.2600590523.

[29] C. Köster, P. Kleinebudde, Evaluation of binders in twin-screw wet granulation – Optimization of tabletability, Int. J. Pharm. 659 (2024). https://doi.org/10.1016/j.ijpharm.2024.124290.

[30] C.C. Sun, H. Hou, P. Gao, C. Ma, C. Medina, F.J. Alvarez, Development of a High Drug Load Tablet Formulation Based on Assessment of Powder Manufacturability: Moving Towards Quality by Design, J. Pharm. Sci. 98 (2009) 239–247. https://doi.org/10.1002/jps.

[31] O. Arndt, R. Baggio, A.K. Adam, J. Harting, E. Franceschinis, P. Kleinebudde, Impact of Different Dry and Wet Granulation Techniques on Granule and Tablet Properties: A Comparative Study, J.

Pharm. Sci. 107 (2018) 3143–3152. https://doi.org/10.1016/j.xphs.2018.09.006.

[32] D. Khan, M. Qindeel, N. Ahmed, M. Imran, Development of an intelligent , stimuli-responsive transdermal system for efficient delivery of Ibuprofen against rheumatoid arthritis, Int. J. Pharm. 610 (2021) 121242. https://doi.org/10.1016/j.ijpharm.2021.121242.

[33] USP42-NF37, <1251>Ibuprofen Tablets, 2021.

[34] O. Taratula, O.B. Garbuzenko, A.M. Chen, T. Minko, Innovative strategy for treatment of lung cancer: targeted nanotechnology-based inhalation co-delivery of anticancer drugs and siRNA, J. Drug Target. 19 (2011) 900–914. https://doi.org/10.3109/1061186X.2011.622404.

[35] A. Kumar, M. Alakarjula, V. Vanhoorne, M. Toiviainen, F. De Leersnyder, J. Vercruysse, M. Juuti, J. Ketolainen, C. Vervaet, J. Paul, K. V Gernaey, T. De Beer, I. Nopens, Linking granulation performance with residence time and granulation liquid distributions in twin-screw granulation: An experimental investigation, Eur. J. Pharm. Sci. 90 (2016) 25–37. https://doi.org/10.1016/j.ejps.2015.12.021.

[36] A. Kumar, J. Dhondt, J. Vercruysse, F. De Leersnyder, V. Vanhoorne, C. Vervaet, J. Paul, K. V Gernaey, T. De Beer, I. Nopens, Development of a process map : A step towards a regime map for steady-state high shear wet twin screw granulation, Powder Technol. 300 (2016) 73–82. https://doi.org/10.1016/j.powtec.2015.11.067.

[37] S. Lute, R.M. Dhenge, A.D. Salman, Twin screw granulation: Effects of properties of primary powders, Pharmaceutics. 10 (2018). https://doi.org/10.3390/pharmaceutics10020068.

[38] N. Bala, J. Corrigan, J. Meyer, M. Schongut, P. Doshi, K. Iyer, K. Lee, M. Rowland, J.D. Litster, N. Dawson, R.M. Smith, Mechanistic modeling of twin screw wet granulation for pharmaceutical formulations : Calibration , sensitivity analysis , and model-driven workflow, Int. J. Pharm. 659 (2024) 124246. https://doi.org/10.1016/j.ijpharm.2024.124246.

[39] M. Franke, T. Riedel, R. Meier, C. Schmidt, P. Kleinebudde, Comparison of scale-up strategies in twin-screw wet granulation, Int. J. Pharm. 641 (2023) 123052. https://doi.org/10.1016/j.ijpharm.2023.123052.

[40] K.P. Hapgood, R. Amelia, M.B. Zaman, B.K. Merrett, P. Leslie, Improving liquid distribution by reducing dimensionless spray flux in wet granulation-A pharmaceutical manufacturing case study, Chem. Eng. J. 164 (2010) 340–349. https://doi.org/10.1016/j.cej.2010.05.007.

[41] J. Vercruysse, A. Burggraeve, M. Fonteyne, P. Cappuyns, U. Delaet, I. Van Assche, T. De Beer, J.P. Remon, C. Vervaet, Impact of screw configuration on the particle size distribution of granules produced by twin screw granulation, Int. J. Pharm. 479 (2015) 171–180. https://doi.org/10.1016/j.ijpharm.2014.12.071.

[42] C. Portier, K. Pandelaere, U. Delaet, T. Vigh, G. Di Pretoro, T. De Beer, C. Vervaet, V. Vanhoorne, Continuous twin screw granulation: A complex interplay between formulation properties, process settings and screw design, Int. J. Pharm. 576 (2020) 119004. https://doi.org/10.1016/j.ijpharm.2019.119004.

[43] A.A. Barrera Jiménez, K. Matsunami, M. Ghijs, D. Van Hauwermeiren, M. Peeters, F. Stauffer, T. De Beer, I. Nopens, Model development and calibration of two-dimensional population balance model for twin-screw wet granulation based on particle size distribution and porosity, Powder Technol. 419 (2023) 118334. https://doi.org/10.1016/j.powtec.2023.118334.

[44] L. Kotamarthy, A. Dan, S. Karkala, S. Parvani, A.D. Román-Ospino, R. Ramachandran, Twin-Screw Granulation: Mechanistic understanding of the effect of material properties on key granule quality attributes through the analysis of mixing dynamics and granulation rate mechanisms, Adv. Powder Technol. 34 (2023) 104137. https://doi.org/10.1016/j.apt.2023.104137.

[45] R. Meier, Continuous Wet Granulation and Fluid-bed Drying-An Experimental Investigation of a New Revolutionary System, LBB Bohle. (2018). https://api.semanticscholar.org/CorpusID:109926323.

[46] S. Shirazian, M. Kuhs, S. Darwish, D. Croker, G.M. Walker, Artificial neural network modelling of continuous wet granulation using a twin-screw extruder, Int. J. Pharm. 521 (2017) 102–109. https://doi.org/10.1016/j.ijpharm.2017.02.009.

[47] A.S. El Hagrasy, J.R. Hennenkamp, M.D. Burke, J.J. Cartwright, J.D. Litster, Twin screw wet granulation: Influence of formulation parameters on granule properties and growth behavior, Powder Technol. 238 (2013) 108–115. https://doi.org/10.1016/j.powtec.2012.04.035.

[48] R. Sayin, A.S. El Hagrasy, J.D. Litster, Distributive mixing elements: Towards improved granule attributes from a twin screw granulation process, Chem. Eng. Sci. 125 (2015) 165–175. https://doi.org/10.1016/j.ces.2014.06.040.

[49] L. Shi, Y. Feng, C.C. Sun, Initial moisture content in raw material can profoundly influence high shear wet granulation process, Int. J. Pharm. 416 (2011) 43–48. https://doi.org/10.1016/j.ijpharm.2011.05.080.

[50] A.S. El-Hagrasy, J.D. Litster, Granulation Rate Processes in the Kneading Elements of a Twin Screw Granulator, AIChE J. 59 (2013) 4100–4115. https://doi.org/10.1002/aic.

[51] Y. Matsui, Y. Ando, K. Yamamoto, S. Watano, Analysis of microstructure of granules prepared by continuous twin screw granulator using x-ray micro-computed tomography, Chem. Pharm. Bull. 67 (2019) 801–809. https://doi.org/10.1248/cpb.c19-00076.

[52] W. Meng, J. Dvořák, R. Kumar, R. Hofmeister, F. Štěpánek, R. Ramachandran, F.J. Muzzio, Continuous high-shear granulation: Mechanistic understanding of the influence of process parameters on critical quality attributes via elucidating the internal physical and chemical microstructure, Adv. Powder Technol. 30 (2019) 1765–1781. https://doi.org/10.1016/j.apt.2019.04.028.

[53] M.B. MacKaplow, L.A. Rosen, J.N. Michaels, Effect of primary particle size on granule growth and endpoint determination in high-shear wet granulation, Powder Technol. 108 (2000) 32–45. https://doi.org/10.1016/S0032-5910(99)00203-X.

[54] N. Rahmanian, M. Ghadiri, Y. Ding, X. Jia, ASSESSMENT OF METHODOLOGIES FOR SCALING-UP OF HIGH SHEAR MIXER ASSESSMENT OF METHODOLOGIES FOR SCALING-UP OF HIGH, in: Proceedings-RELPOWFLOIV, 2008: pp. 528–533.

Table captions

Table 1. Dimensions of the two screw granulators

Table 2. Levels of independent variables

Table 1. Dimensions of the two screw granulators

	D_0 [mm]	D [mm]	c_i [mm]	T [mm]	L_u /D [—]
Ph 11	11.0	10.7	0.15	2.38	25.75
QbCon	25.5	25.0	0.25	4.20	20.00

D_0: barrel diameter; D: screw diameter; c_i: screw to barrel clearance; T: trough; L_u/D: length to diameter ratio used in this work.

Table 2. Levels of independent variables

	Ph 11			**QbCon**		
	LEVELS			LEVELS		
FACTORS	-1	0	1	-1	0	1
LSR	0.2	0.3	0.4	0.2	0.3	0.4
TP (Kg/h)	0.7	0.9	1.1	0.7	1.2	1.7
N (rpm)	250	350	450	180	250	320
$\dot{\gamma}_r$ (s^{-1})	934	1307	1681	942	1309	1676

Figure captions

Figure 1: a) D_{50} dependance with LSR. The red squares represent the Ph 11, while the blue circles the QbCon. The shadow areas correspond to the regions where the best fitted equation would exist. The fitting equation is a hyper-surface that, when projected into the 2D graph of Figure 1, corresponds to the region represented by the shadow area. It is worth noting that the shaded area is not a confidence interval, but with no clear dependance of its variation with other parameters, it might be taken as the D_{50} variability. b) D_{50} normalized as a function of trough (T) size (2.38 mm for Ph11 and 4.20 mm for QbCon).

Figure 2: Span dependence with LSR. The red squares and blue circles correspond to the Ph 11and QbCon, respectively. The shadow areas relate to the regions where the fitted equations exist. The corresponding equations are given in the supplementary material.

Figure 3: Fraction of fines and over-granulated material a) Ph 11 and b) QbCon. The shaded areas correspond to the range of the model fitting equations reported in the supplementary material.

Figure 4: Porosity ε as function of LSR, red squares and blue circles correspond to the Ph 11 and QbCon, respectively. The shadows areas correspond to the region where the fitted equations exist.

Figure 5. Relationship between each DoE responses and tablet tensile strength. a) tensile strength as a function of D_{50}. b) tensile strength as a function of porosity.

Figure 6. Yield (%, fraction of granules within the 125-2000 µm size range) vs. LSR for both granulators.

Figure 7: D_{50}/T as function of S_{max}. Red squares represent the Ph 11 while blue circles represent the QbCon. Different fillings indicate the three different LSR levels.

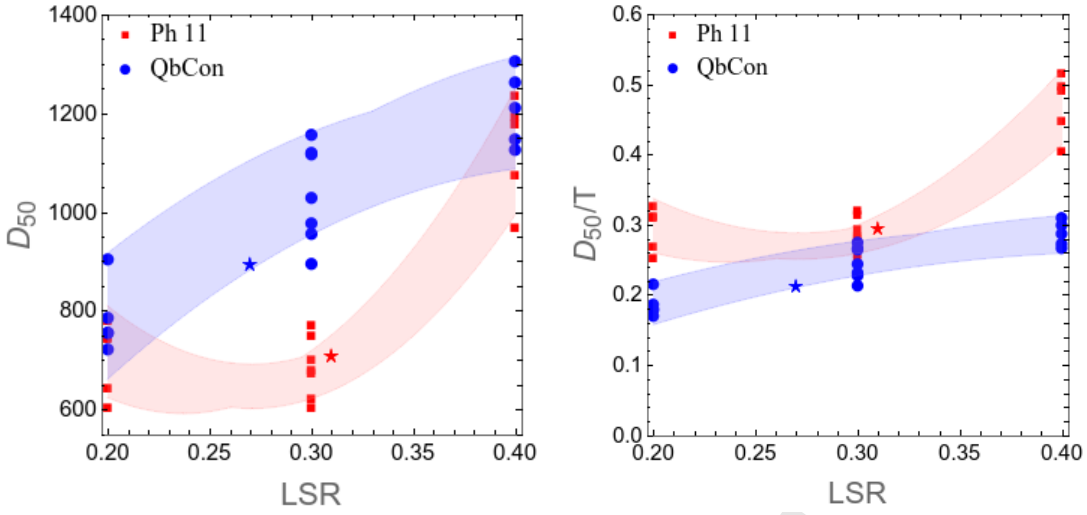

Figure 1: a) D_{50} dependance with LSR. The red squares represent the Ph 11, while the blue circles the QbCon. The shadow areas correspond to the regions where the best fitted equation would exist. The fitting equation is a hyper-surface that, when projected into the 2D graph of Figure 1, corresponds to the region represented by the shadow area. It is worth noting that the shaded area is not a confidence interval, but with no clear dependance of its variation with other parameters, it might be taken as the D_{50} variability. b) D_{50} normalized as a function of trough (T) size (2.38 mm for Ph11 and 4.20 mm for QbCon).

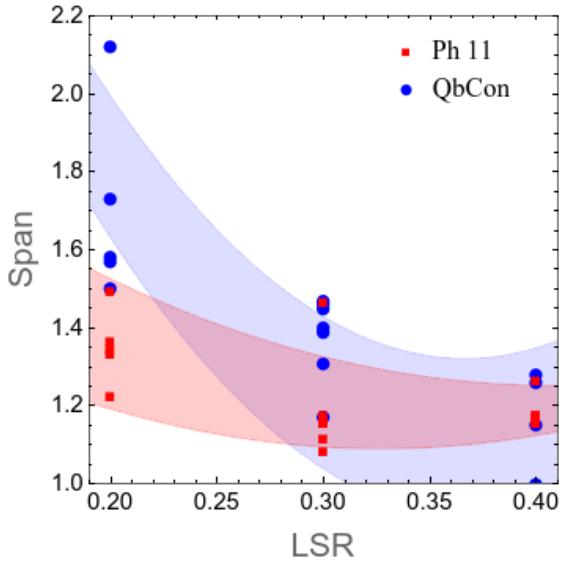

Figure 2: Span dependence with LSR. The red squares and blue circles correspond to the Ph 11and QbCon, respectively. The shadow areas relate to the regions where the fitted equations exist. The corresponding equations are given in the supplementary material.

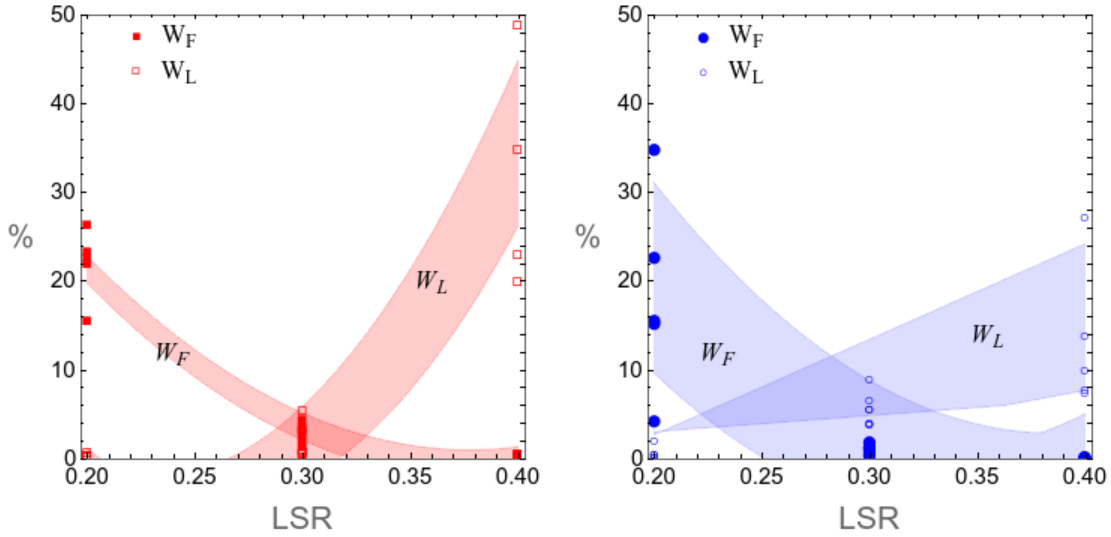

Figure 3: Fraction of fines and over-granulated material a) Ph 11 and b) QbCon. The shaded areas correspond to the range of the model fitting equations reported in the supplementary material.

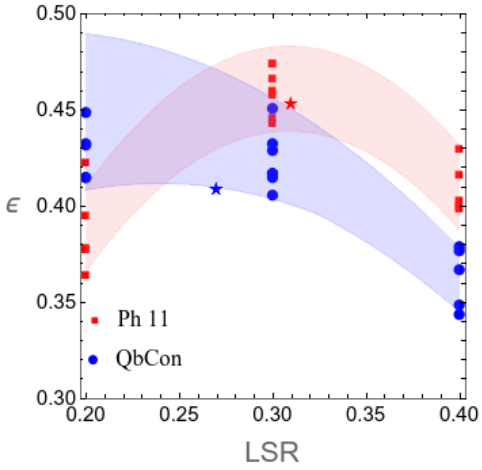

Figure 4: Porosity ε as function of LSR, red squares and blue circles correspond to the Ph 11 and QbCon, respectively. The shadows areas correspond to the region where the fitted equations exist.

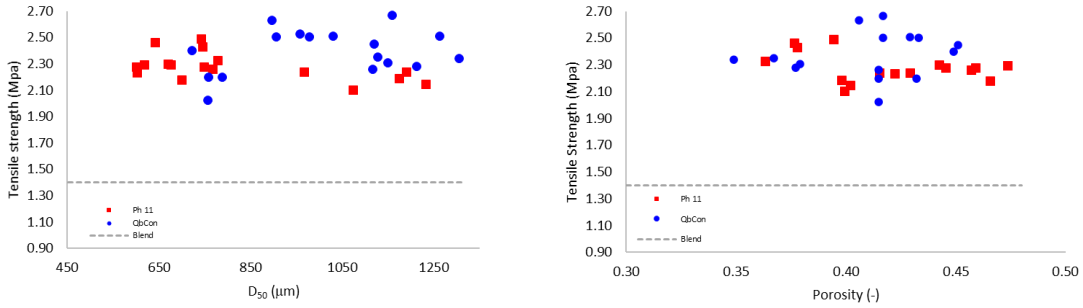

a b

Figure 5. Relationship between each DoE responses and tablet tensile strength. a) tensile strength as a function of D_{50}. b) tensile strength as a function of porosity.

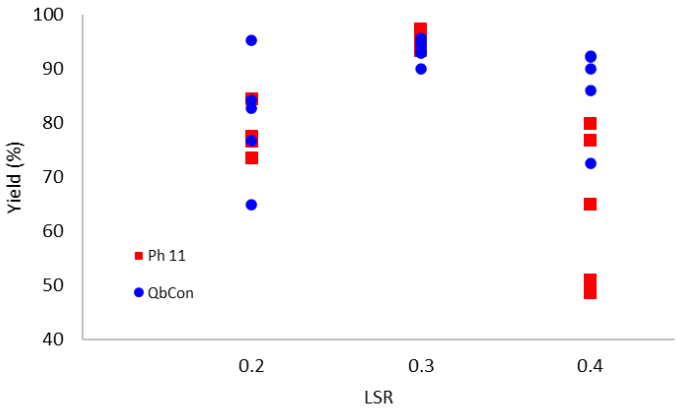

Figure 6. Yield (%, fraction of granules within the 125-2000 µm size range) vs. LSR for both granulators.

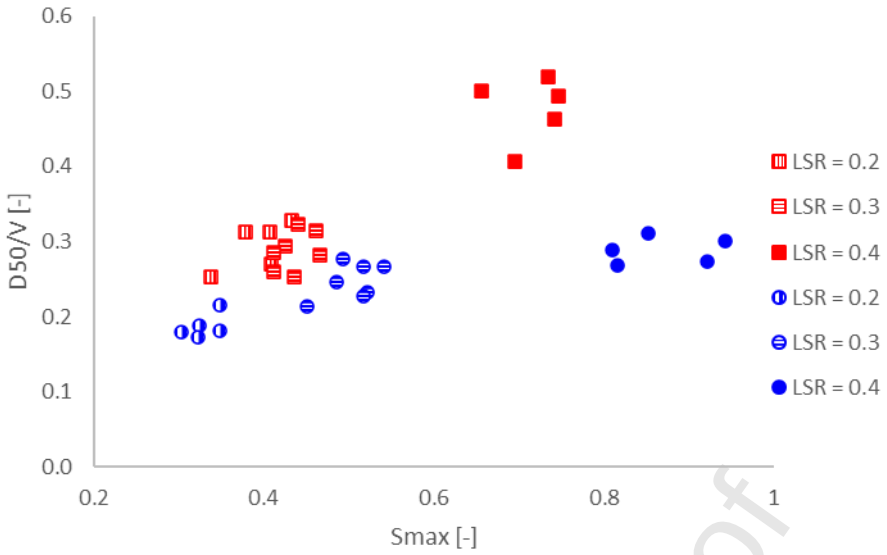

Figure 7: D_{50}/T as function of S_{max}. Red squares represent the Ph 11 while blue circles represent the QbCon. Different fillings indicate the three different LSR levels.

Declaration of interests

☒The authors declare that they have no known competing financial interests or personal relationships that could have appeared to influence the work reported in this paper.

☐The authors declare the following financial interests/personal relationships which may be considered as potential competing interests:

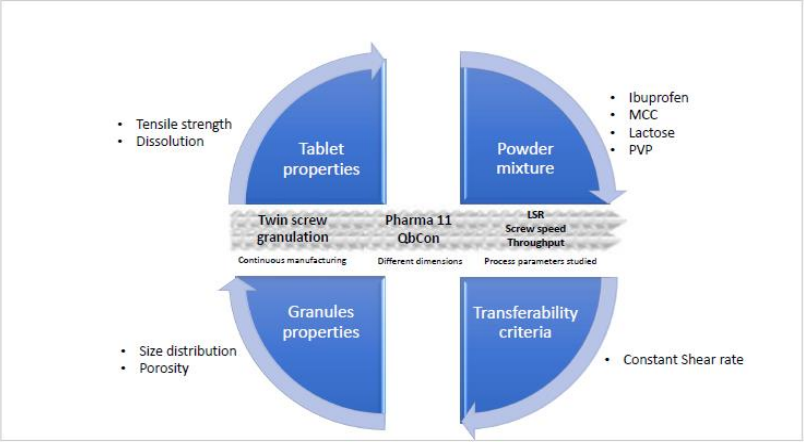

Highlights

- Granules produced at two twin screw granulators using a DoE were compared.
- Ibuprofen content uniformity was consistent across both systems.
- Moderate liquid-to-solid ratio maximizes porosity and usable granules.
- Distinct granule properties observed, yet tablet tensile strength remains comparable.